EPR spectra and magnetization of Eu²⁺ ions in PbSe

S. Isber, S. Charar, C. Fau, V. Mathet, and M. Averous

Groupe d'Etude des Semiconducteurs URA 357, Université Montpellier II, Place Eugene Bataillon, 34095 Montpellier Cedex 5, France

Z. Golacki

Institute of Physics, Polish Academy of Sciences, Pl. 02-668 Warsaw, Poland

Electron-paramagnetic-resonance (EPR) experiments are performed on $Pb_{1-x}Eu_xSe$ at room temperature and at liquid-helium temperature to identify the different transitions with respect to the central one ($\frac{1}{2} \leftrightarrow -\frac{1}{2}$) and to deduce the effective Landé factor g. We found $g = 1.982 \pm 0.002$. The fine structure is in agreement with the crystal-field-level splitting (to second order in perturbation theory). The crystal-field coefficients b_4 and b_6 are found to be, respectively, $b_4 = +269.2$ MHz and $b_6 = -2.4$ MHz at 4.2 K. Furthermore, forbidden transitions and transitions due to pairs are observed. The analysis of magnetization and susceptibility experiments in terms of a modified cluster model of the $Pb_{1-x}Eu_xSe$ shows two types of pairs with different interactions: the first type is attributed to ferromagnetic interactions between the Eu^{2+} ions' nearest neighbors with a constant exchange value of $J_1/k_B = +0.52$ K, and the second is attributed to antiferromagnetic interactions between next-nearest neighbors with a $J_2/k_B = -0.32$ K.

I. INTRODUCTION

To date, diluted magnetic semiconductors have been prepared using II-VI and IV-VI materials. In II-VI compounds, extensive studies have been performed using Mn magnetic ions;[1-4] however, some investigations have been carried out with Fe and Co.[5-10] Also, some work has been done in the case of IV-VI compounds using transition metals and rare earths as magnetic ions. These compounds have attracted attention because they permit a study of the effects of the incorporation of ions with partially filled $3d$ or $4f$ shells in the cubic rock-salt structure rather than the zinc-blende structure. In addition, it is easier to introduce Eu in this structure, because EuSe and EuTe have the cubic rock-salt lattice. Magnetic properties of IV-VI chalcogenides containing magnetic ions have been studied recently. Mathur *et al.*[11] have measured the magnetic susceptibility of $Sn_{1-x}Eu_xTe$ and observed a weak antiferromagnetic coupling between Eu ions. Savage and Rhyne[12] and Anderson *et al.*[13] have measured the magnetization and the magnetic susceptibility of $Pb_{1-x}Gd_xTe$ and found a small antiferromagnetic exchange interaction. Gorska *et al.*[14] performed the same experiments on $Pb_{1-x}Eu_xTe$ and again found a weak antiferromagnetic coupling among Eu ions.

No work, up to date, has been done on $Pb_{1-x}Eu_xSe$. It is probably due to the rather complicated magnetic phase diagram of EuSe (Refs. 15 and 16) which presents several magnetic phases in a small temperature range. In this material the exchange constants J_1 and J_2, which are the exchange interactions between the nearest neighbors (NN) and the next-nearest neighbors (NNN), respectively, are of opposite sign but the same absolute value. It could be expected that in $Pb_{1-x}Eu_xSe$ the interpretation of magnetic measurements, and electron paramagnetic resonance (EPR) will be more difficult than in the previous case. In this paper we try to understand the magnetic interactions between Eu ions, and thus we present experimental results and the analysis of the EPR spectra in the X band (9.56 GHz), the low-field susceptibility, and the high-field (0–70 kOe) magnetization measurements of $Pb_{1-x}Eu_xSe$ ($x \approx 0.03$).

II. EXPERIMENTAL TECHNIQUES

Experiments were carried out on an *n*-type single crystal of $Pb_{1-x}Eu_xSe$, grown by the Bridgman method. The crystal was not intentionally doped with any other element. The solubility limit of Eu in the PbSe matrix is about 10%. X-ray diffraction analysis indicates a fcc structure for all samples. The EPR measurements in the X band (9.56 GHz) were performed on a parallelepidic sample ($3 \times 2.9 \times 2$ mm³) with the longest axis along the [001] direction with a nominal Eu composition of $x = 0.013$. Magnetization measurements (1.5 and 4.2 K) and magnetic susceptibility (1.5–130 K) were performed on three half-disk samples (the diameter $\phi = 8$ mm and the thickness $e = 1$ mm) with a superconducting quantum interference device system at L. Néel Laboratory in Grenoble. For magnetization, the magnetic field varies from 0 up to 70 kOe, whereas the magnetic susceptibility is obtained in the linear part of magnetization ($H \approx 5$ kOe).

III. ELECTRON SPIN RESONANCE

The spin Hamiltonian which describes the electronic states of the ground state $^8S_{7/2}$ in the case of Eu^{2+} $4f^7$, in a cubic crystal field is given by[17-19]

$$H = g\mu_B H \cdot S + B_4(O_4^0 + 5O_4^4) + B_6(O_6^0 - 21O_6^4) + A I \cdot S ,$$

$$(1)$$

where O_4 and O_6 are the fourth and sixth degree cubic operators; b_4 and b_6 are the crystal-field coefficients $(b_4=60\ B_4,\ b_6=1260\ B_6)$, $A\textbf{I}\cdot\textbf{S}$ describes the hyperfine structures for the ^{151}Eu isotope. At zero field, the $L=0$ and $S_0=\frac{7}{2}$ state splits into two doublets Γ_6 and Γ_7 and one quadruplet Γ_8, with the following respective energies (twofold Γ_7 taken as energy origin$=0$):

$$E(\Gamma_6)=32b_4-8b_6\ ,$$

$$E(\Gamma_8)=20b_4+28b_6\ .$$
(2)

It can be deduced that, for $L=0$, there is no crystal-field effect at first order. The allowed transitions are those for which $\Delta m=\pm1$, where m is projection of the angular momentum parallel to the magnetic field. Their positions to second-order correction for the [001] direction are known.[19]

Figure 1 shows the Pb$_{1-x}$Eu$_x$Se $(x=0.013)$ EPR spectrum for $H\|$[001] direction at 4.2 K. The deduced effective Landé factor is $g=1.982\pm0.002$. The symmetrical transitions on each side of the central structure $(\frac{1}{2}\leftrightarrow-\frac{1}{2})$ are easily identified. The crystal-field coefficients are also deduced from the spectrum of Fig. 1: $b_4=+271.5$ MHz; $b_6=-4.1$ MHz at 290 K and $b_4=+269.2$ MHz; $b_6=-2.4$ MHz at 4.2 K. The signs of the crystal-field coefficients b_4 and b_6 are individually determined. As a matter of fact at low temperature $(k_BT<E)$ the population of the m positive value energy levels decreases and then their intensities are less than those corresponding to the m negative values. The energy level positions for Γ_6 and Γ_8 are determined with a good precision with Γ_7 as the origin: $E(\Gamma_6)=(-35.57\pm0.1)\times10^{-6}$ eV; $E(\Gamma_8)=(-21.98\pm0.1)\times10^{-6}$ eV. The observed line shape of the allowed

transitions are Dysonian (except $\pm\frac{7}{2}\leftrightarrow\pm\frac{5}{2}$). This might be due to a skin effect related to an electrical conductivity of the material.[20,21] Resonances $\pm\frac{7}{2}\leftrightarrow\pm\frac{5}{2}$ in Fig. 1 are much wider than other resonances, and the line shape is not Dysonian. These features may be explained by assuming a distribution of $E(\Gamma_6)$ and $E(\Gamma_7)$ values for the Eu^{2+} in the sample. The observed resonance is a superposition of slightly displaced resonances from many spins with different $E(\Gamma_6),E(\Gamma_7)$ tends to make the observed line shape less Dysonian as verified by computer simulations.[20] Nuclear spins are both $I=\frac{5}{2}$ and we get the hyperfine coupling constant $A=120.5$ MHz for the ^{151}Eu isotope deduced from the inset in Fig. 1.

Figure 2 shows the angular dependence of magnetic-field resonance at 290 K, where θ is the angle between the applied magnetic field and the [100] axis when the crystal rotates around the [001] direction. The full lines are calculated and the symbols are the experimental points. The experimental intensities corresponding to the first-order transitions and their theoretical values calculated from Abragam theory[17] are in good agreement. For instance, the experimental integrated intensity ratio of $\frac{1}{2}\leftrightarrow-\frac{1}{2}$ to the $-\frac{3}{2}\leftrightarrow-\frac{1}{2}$ transitions is approximately 16:12.4 instead of the theoretical 16:15. However, two forbidden transitions $(\Delta m=\pm2)$ are observed, $\frac{7}{2}\leftrightarrow\frac{3}{2}$ and $\frac{3}{2}\leftrightarrow-\frac{1}{2}$ at 4.2 K, and these identifications are in good agreement with the crystal-field coefficients $(b_4$ and $b_6)$ which are deduced from the spectrum $H\|$[001] in Fig. 1. The observed structures in the range 3.6–4.2 kOe do not fit with transitions due to single ions $(L=0,\ S_0=\frac{7}{2})$ for any Δm. Probably these structures are caused by transitions due to pairs. The total Hamiltonian of a pair could be
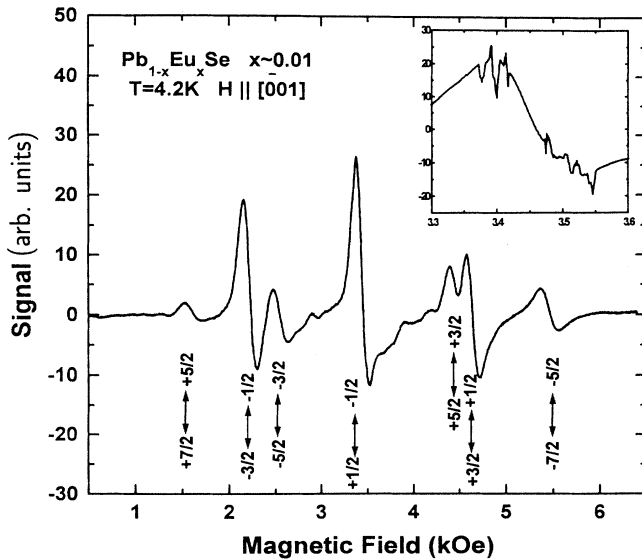

FIG. 1. EPR spectrum Eu^{2+} in PbSe for $H\|$[001] at 4.2 K. The enlarged scale shows the central line and reveals the hyperfine structure.
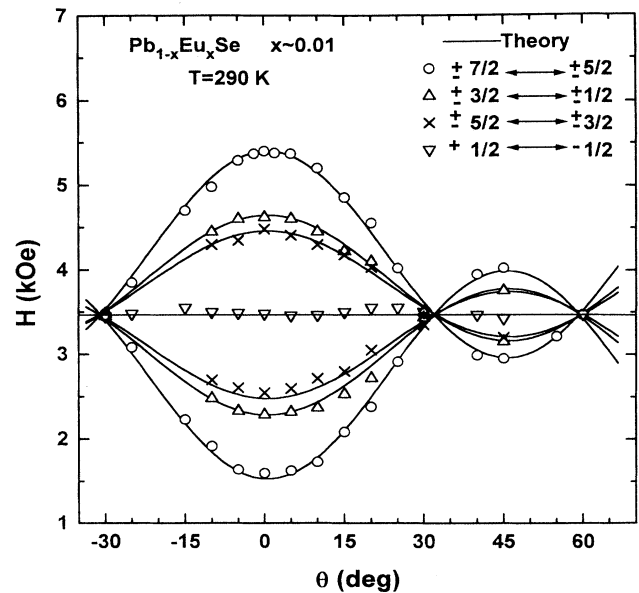

FIG. 2. Rotation diagram (i.e., resonance field as a function of the angle between H and the [001] axis) of Eu^{2+} at 290 K. Symbols, experiment; solids lines, calculated with the parameters given in the text.

written as

$$\mathbf{H}_p = g\mu_B \mathbf{H} \cdot (\mathbf{S}_1 + \mathbf{S}_2) - 2J_p \mathbf{S}_1 \cdot \mathbf{S}_2 + B_4(O_4^0 + 5O_4^4)$$
$$+ B_6(O_6^0 - 21O_6^4) . \tag{3}$$

We have not observed any anisotropy on the obtained structures as a function of θ between 3.6 and 4.2 kOe, so the crystal field has been neglected and these structures are assumed as only due to the isotropic exchange in the pairs J_p. The pair energy levels are calculated from[8,22]

$$E_p(S_T, m) = -mg\mu_B H + J_p[S_T(S_T+1) - 2S_0(S_0+1)] , \tag{4}$$

where $0 \le S_T \le 2S_0$, $-S_T \le m \le S_T$, and $S_0 = \frac{7}{2}$.

If we introduce $J_p/k_B = 0.52$ K determined from magnetization in Eq. (5), at 4.2 kOe we obtained, for instance, $E_p(1,1) - E_p(0,0) = 9.9$ GHz which corresponds roughly to the frequency used in this experiment (9.56 GHz).

IV. MAGNETIZATION AND MAGNETIC SUSCEPTIBILITY

Figures 3(a) and 3(b) show magnetization vs magnetic field for sample 1 at 1.5 and 4.2 K, respectively; samples 2 and 3 behave like sample 1. The experimental points are the open circles; the full lines are calculated using the "modified cluster model":[23-25]

$$M_t = M_s + M_{p1} + M_{p2} + M_{ot1} + M_{ct1} + M_{ot2} + M_\chi , \tag{5}$$

where M_s, M_{p1}, M_{p2}, M_{ot1}, M_{ct1}, and M_{ot2} are the contributions to the magnetization of the singles, the NN pairs, the NNN pairs, the NN open triangles, the NN closed triangles, and the NNN open triangles, and M_χ is the PbSe lattice diamagnetic contribution with $\chi_0 = -3.6 \times 10^{-7}$ emu/g Oe.[13,18] The contribution of the singles is given by[14]

$$M_s = M_o S_0 x_{SAT} B_{s0}(\xi) , \tag{6}$$

where $M_o = g\mu_B N_A/m(x_{SAT})$. N_A is the Avogadro number, k_B is the Boltzmann constant, μ_B is the Bohr magneton, $m(x_{SAT})$ is the molar mass of the compound, $m(x_{SAT}) = (1 - x_{SAT})m_{Pb} + x_{SAT} m_{Eu} + m_{Se}$, x_{SAT} is the
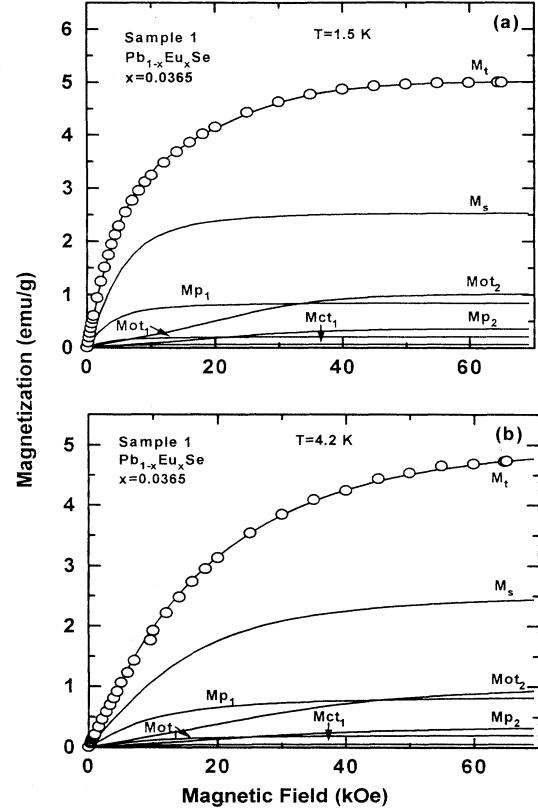

FIG. 3. Magnetization for sample 1 vs magnetic field. (a) at 1.5 K; (b) at 4.2 K. Symbols, experiment; solids lines, calculated from isolated ions NN pairs NNN pairs; and triangles: contributions.

mole fraction of Eu^{2+} determined from the saturation of the magnetization, $B_{s0}(\xi)$ is the Brillouin function:

$$B_{s0}(\xi) = \frac{2S_0+1}{2S_0}\coth\left[\frac{2S_0+1}{2S_0}\xi\right] - \frac{1}{2S_0}\coth\left[\frac{\xi}{2S_0}\right] , \tag{7}$$

where $\xi = S_0 g\mu_B H/k_B T$. The pairs contribution is[21,26]

$$M_{Pi} = \frac{1}{2}M_o x_i \frac{\sum\limits_{S=0}^{S_{max}} \exp\left[\frac{J_i}{k_B T}S(S+1)\right]S\left[\sinh\left(\frac{2S+1}{2S}\xi_P\right)\right]B_S(\xi_P)}{\sum\limits_{S=0}^{S_{max}} \exp\left[\frac{J_i}{k_B T}S(S+1)\right]\left[\sinh\left(\frac{2S+1}{2S}\xi_P\right)\right]} , \quad i=1,2 , \tag{8}$$

with $\xi_P = Sg\mu_B H/k_B T$ and $S_{max} = 2S_0$. And the triangle contributions for open and closed triangles are, respectively,

$$M_{oti} = M_0 P_{oti}\langle S_z \rangle_{oti}, \quad i=1,2 , \tag{9}$$
$$M_{ct1} = M_0 P_{ct1}\langle S_z \rangle_{ct1} ,$$

with

$$\langle S_z \rangle_{oti} = \frac{\sum\limits_{S_a,S_b,m} m\exp[-E_{oti}(S_a,S_b,m)/k_B T]}{\sum\limits_{S_a,S_b,m} \exp[-E_{oti}(S_a,S_b,m)/k_B T]} \tag{10}$$

and

$$E_{oti} = -mg\mu_B H + J_i[S_b(S_b+1) - S_a(S_a+1)$$
$$-S_0(S_0+1)], \quad i=1,2 , \qquad (11)$$

$$0 \le S_a \le 7, \quad |S_a - \tfrac{7}{2}| \le S_b \le S_a + \tfrac{7}{2}, \quad |m| \le S_b ,$$

$$\langle S_z \rangle_{ct1} = \frac{\displaystyle\sum_{S_a,S_b,m} m \exp[-E_{ct1}(S_a,S_b,m)/k_B T]}{\displaystyle\sum_{S_a,S_b,m} \exp[-E_{ct1}(S_a,S_b,m)/k_B T]} , \qquad (12)$$

$$E_{ct1} = -mg\mu_B H + J_1[S_b(S_b+1) + 3S_0(S_0+1)] . \qquad (13)$$

The probabilities to find magnetic ions in a single or pair or triangle situation are, respectively,[27]

$$P_s = (1-x_{SAT})^{18}, \quad P_{ot1} = 90x_{SAT}^2(1-x_{SAT})^{34} ,$$

$$P_{p1} = 12x_{SAT}(1-x_{SAT})^{26} ,$$

$$P_{ct1} = 24x_{SAT}^2(1-x_{SAT})^{31} ,$$

$$P_{p2} = 6x_{SAT}(1-x_{SAT})^{30} , \qquad (14)$$

$$P_{ot2} = 1 - P_s - P_{p1} - P_{p2} - P_{ot1} - P_{ct1} .$$

The results of the three samples are given in Table I. Consequently the fitting model used in this work is a two-fitting-parameter model, namely, J_1 and J_2, which are the exchange constants in NN and NNN pairs. It could be observed that J_1 is ferromagnetic ($J_1 > 0$) and J_2 antiferromagnetic ($J_2 < 0$). This result is in agreement with the susceptibility measurements performed between 4 and 130 K. In Fig. 4 (sample 1), χ^{-1} vs T, when the diamagnetic contribution χ_0 is removed, follows a Curie-Weiss law, with a slope change at about 50 K which confirms the existence of two types of interactions. In the range $T > 50$ K the corresponding Curie-Weiss behavior gives a θ_1 value > 0, whereas for $T < 50$ K θ_2 is negative. The Curie-Weiss constant could be written as follows:[23]

$$\theta(x) = [2xS_0(S_0+1)/3k_B] \sum_{i=1,2} Z_i J_i , \qquad (15)$$

Z_i is the number of sites on the sphere. In this case, $Z_1 = 12$ and $Z_2 = 6$:

$$\theta_1(x_{SAT}) = [2x_{SAT}S_0(S_0+1)/3k_B]Z_1 J_1 ,$$

$$\theta_2(x_{SAT}) = [2x_{SAT}S_0(S_0+1)/3k_B]Z_2 J_2 .$$

Using the J_1/k_B and J_2/k_B values deduced from magnetization, we have calculated the inverse magnetic suscep-

TABLE I. x_{SAT}, J_1/k_B, and J_2/k_B for samples 1, 2, and 3, deduced from magnetization.

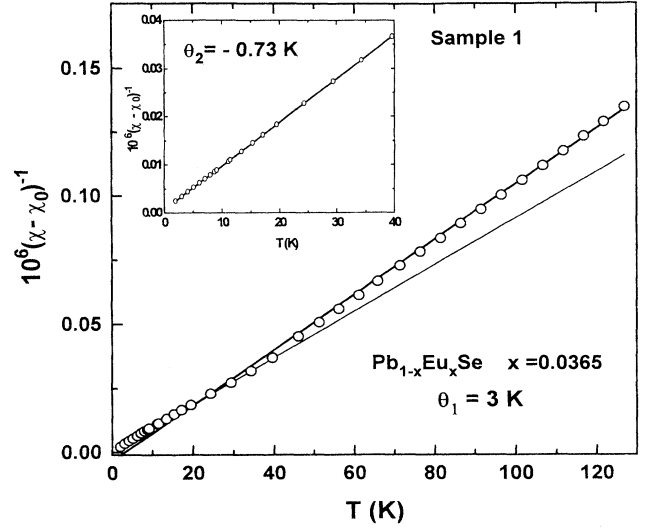| Sample	T (K)	x_{SAT}	J_1/k_B (K)	J_2/k_B (K)
1	1.5	0.0365	0.52	−0.32
	4.2		0.52	−0.33
2	1.5	0.0372	0.51	−0.32
	4.2		0.52	−0.31
3	1.5	0.033	0.54	−0.30
	4.2		0.52	−0.31

FIG. 4. Inverse susceptibility vs temperature for sample 1. The enlarged scale shows a linear behavior at lower T. Symbols, experiment; solids lines, calculated.

tibility vs temperature. The calculated curve fits well with the experimental data, showing clearly the two slopes corresponding to the two kinds of magnetic interactions. We have chosen the model with the singles, the NN pairs, the NNN pairs, and different types of triangles in order to introduce J_1 and J_2, for two reasons: The first one is the knowledge of J_1 and J_2 in the magnetic semiconductors EuSe, in which the bond lengths Eu-Se are the same as in Pb$_{1-x}$Eu$_x$Se; the second one is due to the observed dependence of χ^{-1} which shows two behaviors depending on the temperature range.

However, a fitting of the magnetization, taking into account the isolated ions and only one kind of pair, namely, with antiferromagnetic interactions, with an appropriate phenomenological parameter T_0, works as well as the proposed model. That means that one cannot make a conclusion only by the magnetization experiments, since the fit is not unique. One needs at least magnetization and susceptibility to select the good physical approximation.

V. CONCLUSION

By using a modified cluster model we have shown in Pb$_{1-x}$Eu$_x$Se that the magnetization and the susceptibility could be interpreted by $J_1/k_b = 0.52$ K and $J_2/k_b = -0.32$ K. The role of J_1 is very important. In the case of Pb$_{1-x}$Eu$_x$Te (Ref. 14) the behavior was completely different: J_1 can be neglected with regard to J_2 and the dominant interactions were of an antiferromagnetic type.

From the low-temperature EPR data the allowed transitions and those due to the pairs are identified. The crystal-field coefficients b_4 and b_6 are deduced and the hyperfine structure coupling constant A is found to be 120.5 MHz for ^{151}Eu.

ACKNOWLEDGMENTS

[1]Y. Shapira, S. Foner, P. Becla, D. N. Domingues, M. J. Naughton, and J. S. Brooks, Phys. Rev. B 33, 356 (1986).

[2]M. Gorska and J. R. Anderson, Phys. Rev. B 38, 9120 (1988).

[3]J. K. Furdyna, J. Appl. Phys. 64, R29 (1988).

[4]Semimagnetic Semiconductors and Diluted Magnetic Semiconductors, edited by M. Averous and M. Balkanski, Physical Sciences No. 55 (Plenum, New York, 1991), and references therein.

[5]A. Lewicki, J. Spalek, and A. Mycielski, Solid State Phys. 20, 2005 (1987).

[6]A. Twardowski, J. Appl. Phys. 67, 5108 (1990).

[7]A. Lewicki, A. I. Schindler, I. Miotkowski, and J. K. Furdyna, Phys. Rev. B 41, 4653 (1990).

[8]T. Q. Vu, V. Bindilatti, Y. Shapira, E. J. McNiff, C. C. Agosta, J. Papp, R. Kershaw, K. Dwight, and A. Wold, Phys. Rev. B 46, 11 617 (1992).

[9]M. Averous, C. Fau, S. Charar, M. El Kholdi, V. D. Ribes, and Z. Golacki, Phys. Rev. B 47, 10 261 (1993).

[10]V. Bindilatti, A. N. Anisinov, N. F. Olivera, Y. Shapira, M. Goiran, F. Yang, S. Isber, M. Averous, and M. Demianiuk, Phys. Rev. B 50, 16 464 (1994).

[11]M. P. Mathur, D. W. Deis, K. Jones, A. Patterson, and W. J. Carr, J. Appl. Phys. 42, 1693 (1971).

[12]H. T. Savage and J. J. Rhyne, in Proceedings of the 17th Annual Conference on Magnetism and Magnetic Material, Chicago, 1971, edited by D. C. Graham and J. J. Rhyne, AIP Conf. Proc. No. 5 (American Institute of Physics, New York, 1972), p. 879.

[13]J. R. Anderson, G. Kido, Y. Nishina, M. Gorska, L. Kowalczyk, and Z. Golacki, Phys. Rev. B 41, 1014 (1990).

[14]M. Gorska, J. R. Anderson, G. Kido, S. M. Green, and Z. Golacki, Phys. Rev. B 45, 11 702 (1992).

[15]R. Griessen, M. Landolt, and H. R. Ott, Solid State Commun. 9, 2219 (1971).

[16]P. Wachter, in Handbook on Physics and Chemistry of Rare Earths, edited by K. A. Gschneidner and L. Eyring (North-Holland, Amsterdam, 1979).

[17]A. Abragam and B. Bleaney, Electron Paramagnetic Resonance of Transition Ions (Clarendon, Oxford, 1972), Vol. 1.

[18]T. R. McCurie, B. E. Argyle, M. W. Shofer, and J. S. Smart, Appl. Phys. Lett. 1, 17 (1962).

[19]G. B. Bacskay, P. J. Fensham, and I. M. Ritchie, J. Phys. Chem. Solids 29, 1213 (1968).

[20]S. Isber, M. Averous, Y. Shapira, V. Bindilatti, A. N. Anisinov, N. F. Olivera, V. M. Orera, and M. Demianiuk, Phys. Rev. B 51, 15 211 (1995).

[21]M. El Kholdi, M. Averous, S. Charar, C. Fau, G. Brun, H. Ghoumari-Bouanani, and J. Deportes, Phys. Rev. B 49, 1711 (1994).

[22]Y. Shapira, in Semimagnetic Semiconductors and Diluted Magnetic Semiconductors (Ref. 4), p. 121.

[23]G. Karczewski, M. Von Ortenberg, Z. Wilamowski, W. Dobrowolski, and Niewodniczanska-J. Zawadzka, Solid State Commun. 55, 249 (1985).

[24]S. Nagata, R. R. Galazka, D. P. Mullin, H. Akbarzadeh, G. D. Khattak, J. K. Furdyna, and P. H. Keesom, Phys. Rev. B 22, 3331 (1980).

[25]T. R. McCurie and M. W. Shofer, J. Appl. Phys. 35, 984 (1964).

[26]G. Bastard and C. Lewiner, J. Phys. C 13, 1469 (1980).

[27]M. M. Kreitman and D. L. Barnett, J. Chem. Phys. 43, 364 (1965).